Life cycle assessment of hydrogen-based fuels use in internal combustion engines of container ships until 2050

Wei, S.; Kanchiralla, F.M.; Schulte, F.; Polinder, H.; Tukker, A.; Steubing, B.R.P.

Resources, Conservation & Recycling 226 (2026) 108671

Contents lists available at ScienceDirect

Resources, Conservation & Recycling

journal homepage: www.sciencedirect.com/journal/resources-conservation-and-recycling

Life cycle assessment of hydrogen-based fuels use in internal combustion engines of container ships until 2050

Shijie Wei [a,*], Fayas Malik Kanchiralla [b], Frederik Schulte [c], Henk Polinder [c], Arnold Tukker [a,d], Bernhard Steubing [a]

[a] Institute of Environmental Sciences (CML), Leiden University, 2333 CC Leiden, The Netherlands
[b] Department of Mechanics and Maritime Sciences, Chalmers University of Technology, Hörselgången 4, SE-412 96 Gothenburg, Sweden
[c] Department of Maritime and Transport Technology, Delft University of Technology, Mekelweg 2, 2628 CD Delft, The Netherlands
[d] Netherlands Organization for Applied Scientific Research TNO, 2595 DA The Hague, The Netherlands

ARTICLE INFO

Keywords:
Life cycle assessment
Hydrogen
Ammonia
Methanol
Maritime shipping
Climate change

ABSTRACT

Hydrogen-based fuels are potential candidates to help international shipping achieve net-zero greenhouse gas (GHG) emissions by around 2050. This paper quantifies the environmental impacts of liquid hydrogen, liquid ammonia, and methanol used in a Post-Panamax container ship from 2020 to 2050. It considers cargo capacity changes, electricity decarbonization, and hydrogen production transitions under two International Energy Agency scenarios: the Stated Policies Scenario (STEPS) and the Net Zero Emissions by 2050 Scenario (NZE). Results show that, compared to the existing HFO ship, hydrogen-based propulsion systems can decrease cargo weight capacity by 0.3 % to 25 %. In the NZE scenario, hydrogen-based fuels can reduce GHG emissions per tonne-nautical mile by 48 %–65 % compared to heavy fuel oil by 2050. Even with fully renewable hydrogen-based fuels, 18 %–31 % of GHG emissions would still remain. Using hydrogen-based fuels in internal combustion engines requires attention to minimize environmental trade-offs.

1. Introduction

International shipping enables 80–90 % of global trade and comprises about 85 % of the net greenhouse gas (GHG) emissions associated with the shipping sector (IRENA, 2021). The high amount of GHG emissions is mainly due to high reliance on the use of fossil fuels including heavy fuel oil (HFO) and marine gas oil (MGO) (IMO, 2021b). The International Maritime Organization (IMO) aims to reach net-zero GHG emissions from international shipping close to 2050 and strives to achieve an uptake of 5–10 % alternative zero and near-zero GHG fuels in energy use by 2030 (IMO, 2023). Hydrogen-based fuels like hydrogen (H_2), ammonia (NH_3) and methanol (MeOH) are candidate low-carbon fuels (IRENA 2021; Balcombe et al., 2019; Müller-Casseres et al., 2024). At this moment, the shipping sector has limited experience using H_2-based fuels and overall environmental trade-offs of these different fuels have not yet been extensively analyzed.

Assessing the environmental impacts of using H_2-based fuels on ships helps to identify environmentally optimal alternative fuels and design a comprehensive roadmap to promote an effective transition to low-carbon fuels. Life cycle assessment (LCA) is the standard approach to assess the environmental impacts in a scientific and holistic manner (IMO, 2023). Several studies have done LCA research on using H_2-based fuels for international shipping. Bicer and Dincer (2018) compare the environmental impacts of low-carbon H_2 and NH_3 produced with biomass, municipal waste and geothermal energy and HFO when used for transoceanic freight shipping. They find that switching to low-carbon H_2 and NH_3 in maritime transportation can reduce GHG emissions and other environmental impacts considerably. They assume the energy use per tonne-kilometer is the same among different fuels and ignore, for instance, changes in available cargo capacity due to changes in fuel storage and propulsion systems adapted to the different fuels (Korberg et al., 2021; Kim et al., 2020; Stolz et al., 2022). Kanchiralla et al. (2023) evaluate the environmental impacts of operating a tanker equipped with an internal combustion engine and fuel cell, powered by various hydrogen-based fuels such as H_2, NH_3, and MeOH, by 2030. While the initial technical viability analysis quantifies the changes in volume and weight of H_2-based propulsion systems compared to traditional ones, the effects of possible cargo capacity loss on environmental impacts have

* Corresponding author.
E-mail address: s.j.wei@cml.leidenuniv.nl (S. Wei).

https://doi.org/10.1016/j.resconrec.2025.108671
Received 11 July 2025; Received in revised form 13 September 2025; Accepted 24 October 2025
Available online 31 October 2025

not been comprehensively assessed. Moreover, existing research often assumes that H_2-based fuels are exclusively sourced from renewables or low-carbon electricity, while overlooking the constraints of the global H_2 market, with the market shares of different technologies varying across roadmaps. This assumption could lead to overly optimistic conclusions regarding the decarbonization of the shipping sector using H_2-based fuels.

To fill this knowledge gap, we develop a methodology to quantify the changes in cargo space and weight when replacing traditional HFO propulsion systems with H_2-based fuels. This approach is integrated with a future-oriented global H_2 production model that includes improvements in energy and material efficiency, the evolution of the H_2 market, and electricity decarbonization. Using this framework, the life-cycle environmental impacts of a typical Post-Panamax containership powered by various H_2-based fuels are quantified from 2020 to 2050. The results aim to guide the deployment of H_2-based fuels in container shipping while minimizing environmental impacts.

2. Methods and data

2.1. Goal and scope

An attributional LCA is used in this study to compare the environmental impacts of a containership powered by liquid H_2, liquid NH_3, MeOH, and conventional HFO from cradle-to-grave between 2020 and 2050. The functional unit of this study is defined as "carrying one tonne of cargo over a distance of one nautical mile (t-nm)", where 1 nm equals 1.852 km. A Post-Panamax containership with a capacity of 8749 TEU (twenty-foot equivalent units) is chosen as the representative ship for the size range 8000–11,999 TEU, which is the most commonly used size class for international container shipping (there are nine size categories of containerships, ranging from 0–999 TEU to 20,000+ TEU). Ships within this size class (8000–11,999 TEU) were also the largest emitters of GHG emissions among containerships in 2018, accounting for 25 % of emissions (IMO, 2021b). By 2050, this category is expected to have the largest share of ships, up to 20 % (IMO, 2021b). As shown in Fig. 1, this study considers four types of propulsion systems: diesel internal combustion engines (ICE) burning HFO, and dual fuel ICE using liquid H_2, liquid NH_3, and MeOH with MGO as the pilot fuel. Since H_2-based fuels

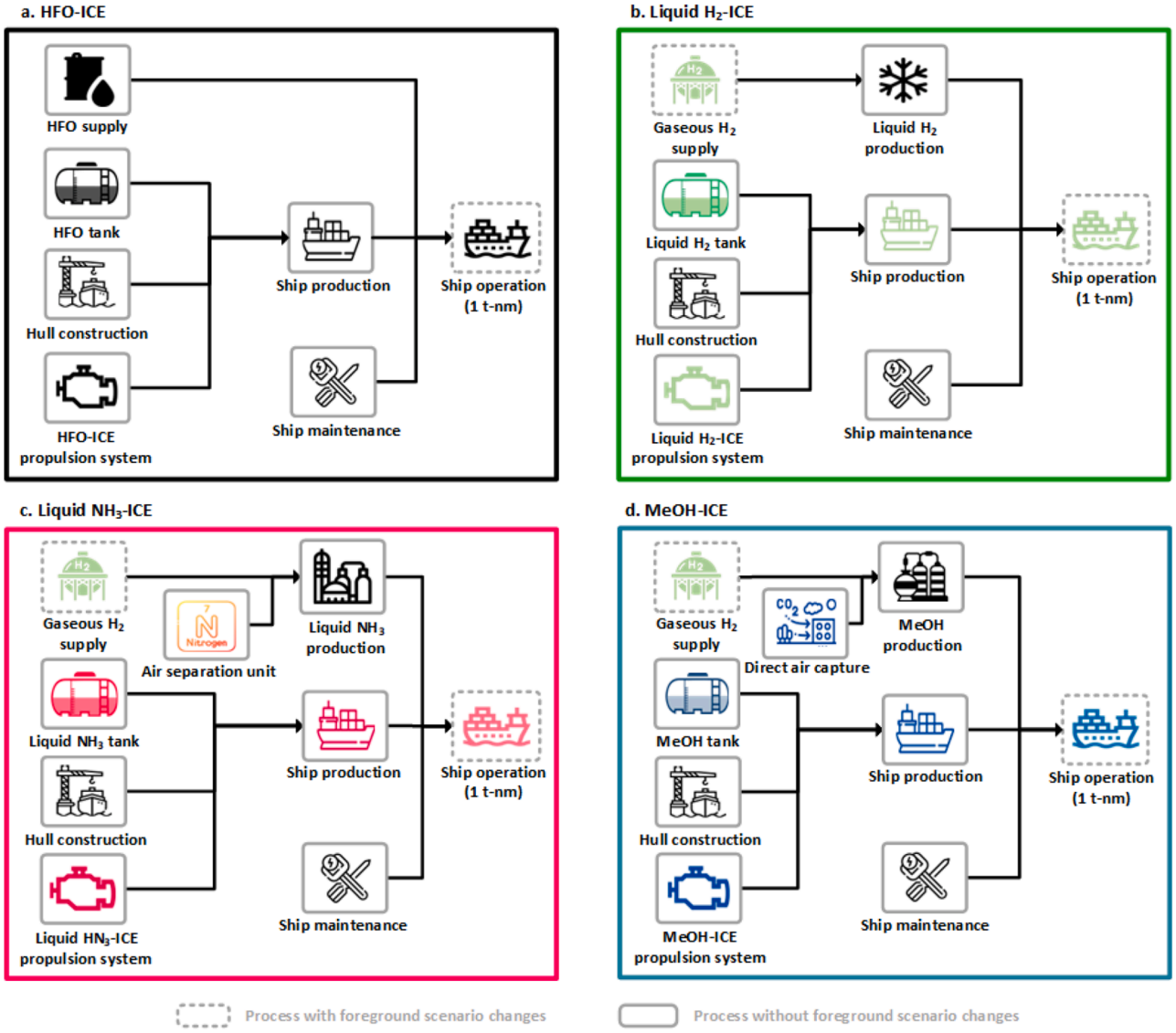

Fig. 1. System boundaries for container shipping with different propulsion systems (The case ship information and detailed flow charts showing the unit processes of each propulsion system are provided in Section 1 of the supporting information (SI)).

are difficult to ignite directly under compression-ignition conditions, a small amount of easily ignitable pilot fuel is required to ignite the primary alternative fuel (IMO, 2021b). Dual fuel ICE are emphasized in the Fourth IMO report because they are easier to scale up compared to spark ignition engine (IMO, 2021b). Additionally, dual fuel ICE can utilize H_2-based fuels with slightly lower energy efficiency compared to traditional diesel ICE; however, they do not require significant retrofitting of existing propulsion systems and offer lower costs compared to fuel cells. For MeOH production, this study considers CO_2 from direct air capture (DAC) as the feedstock. Although biogenic CO_2 can currently be obtained at lower cost, its availability is limited (IRENA, 2021). Moreover, DAC has lower land intensity and greater flexibility in both time and space (Fuhrman et al., 2021; Terlouw et al., 2021), making it a more scalable and globally applicable solution in the long-term.

To comprehensively reflect the impacts of these propulsion systems and corresponding fuel supply on the environment, this study considers multiple ship design and operation scenarios involving different ranges and speeds, as well as future H_2 supply scenarios aligned with different policy settings (see Sections 2.1.1 and 2.2.2). Consistent with the foreground data, background data reflecting electricity decarbonization under different scenarios are also used (see Section 2.2.7).

2.1.1. Ship design and operation scenarios

The various H_2-based propulsion systems differ in overall volume and weight, depending on the configuration of components within the system, the physical properties of each fuel—liquid H_2, liquid NH_3, or MeOH—and the specific tank types designed to storage each fuel. These differences will affect the cargo capacity in terms of available space and weight compared to HFO-ICE ship. The size of the fuel tank is an important aspect of such long-distance vessels which depends on the ship's designed range (a larger fuel tank is required for a larger range, but could affect cargo capacity), and speed (slower speed decreases energy consumption for the same range (Lindstad et al., 2011) and allows for a smaller fuel tank, although it requires more time to complete the journey). The change in the available cargo capacity will directly impact the fuel use per transport work and, consequently, the environmental impacts.

To investigate the impacts of these design and operation choices, the study sets various operation scenarios covering different ranges, speeds, and refueling times. As shown in Table 1, six combined scenarios are analyzed based on a main route between Asia (Shanghai) and Europe (Rotterdam), where container ships with a capacity of 8000–11,999 TEU operate (GMH, 2019, IRENA, 2021). The round trip between Shanghai and Rotterdam without refueling, which is technically feasible but requires carrying more fuel on board at once, serves as the upper boundary. Although the scenario assuming a 22,000 nm round trip without refueling may not reflect typical operational practice, it is included as an exploratory boundary scenario to assess the upper-limit impact of H_2-based fuels on ship cargo capacity. This extreme case is intended to reveal the technical design constraints that may arise under maximum endurance conditions. A typical single trip between Shanghai and Rotterdam covering 11,000 nm range without refueling is set as the medium scenario. Finally, a single trip between Shanghai and Rotterdam with one refueling stop is assumed to represent the minimum operational range of 5500 nm. Interim port calls that allow for refueling can reduce the amount of fuel carried; however, frequent stops also increase operational costs due to port fees and time spent in port. Therefore, only one port call is assumed in this scenario. This shorter route is well within the range of the container ships in this size category (ICCT, 2020). Each range is coupled with an average service speed of 20 nautical miles per hour (knots) (Minnehan and Pratt, 2017) and a lower speed of 16 knots (MI, 2019) to evaluate the effects of speed.

Table 1
Ship operation scenarios. The range refers to the maximum distance a ship can go on a single fuel loadout.

Scenario	R-A-N	R-L-N	S-A-N	S-L-N	S-A-I	S-L-I
Range	22,000 nm	22,000 nm	11,000 nm	11,000 nm	5500 nm	5500 nm
Trip	Round	Round	Single	Single	Single	Single
Speed	20 knots	16 knots	20 knots	16 knots	20 knots	16 knots
Stops to refuel	Nonstop	Nonstop	Nonstop	Nonstop	1	1

2.2. Life cycle inventory analysis

We will now discuss the unit process data for ship production, fuel supply, and ship operation. Detailed information on all unit process data is available in Section 2 of the SI.

2.2.1. Ship production

The material composition of the container ship construction is determined by the lightweight mass (LWT) as calculated by Eq. (1), and material breakdowns are from Jain et al. (2016) and Notten et al. (2018). Material demands for the main engine are excluded at this stage, with detailed life cycle inventory (LCI) data for the main engine collected separately. Welding, electricity use, heat consumption, and emissions during hull construction are calculated according to Notten et al. (2018).

$$LWT = (1-\lambda) \times \frac{DWT}{\lambda} \quad (1)$$

where *LWT* represents the weight of the empty vessel, including hull material, machinery, and outfitting (SRI, 2018); deadweight tonnage (*DWT*) is the load capacity of the vessel, including the cargo, fuel, water, crew and effects (Tupper, 2013) (103,800 t (Scheepvaartwest, 2025)); and λ is the ratio of the *DWT* to the total weight of the ship (70 % (Papanikolaou, 2014)). It is assumed that the *LWT* of the ship remains unchanged regardless of the propulsion system.

2.2.2. H_2 supply

This study builds upon the model of Wei et al. (2024) to account for the environmental impacts of global future H_2 supply, which integrates two H_2 scenarios by the International Energy Agency's, the Stated Policies (STEPS) Scenario and Net Zero Emissions by 2050 (NZE) Scenario (Wei et al., 2024). The models encompass nine leading H_2 production technologies, including coal gasification, natural gas steam reforming, and biomass gasification, both with and without carbon capture and storage (CCS), as well as grid-coupled water electrolysis using alkaline electrolyzers, proton exchange membrane electrolyzers, and solid oxide electrolysis cells. The models also consider electricity decarbonization, efficiency improvements, advancements in electrolyzer technology, and changes in the H_2 production mix.

2.2.3. Fuel oil and H_2-based fuel supply chain

The HFO and MGO are sourced from the global market as modeled in the ecoinvent database (Wernet et al., 2016). To comply with the global sulfur limit outside Sulfur Emission Control Areas (SECAs) under the IMO 2020 regulation (IMO, 2021a), a desulfurization process based on Silva (2017) is applied to reduce the sulfur content in HFO and MGO from 1.03 % (Wernet et al., 2016) to 0.5 %. Although SECAs enforce a stricter sulfur content limit of 0.1 %, and fuel switching is required when entering these areas, this process is not considered in the model since the fuel consumption within SECAs is marginal compared to the total voyage. The gaseous H_2 from the global market (Wei et al., 2024) is used as the feedstock for the liquid H_2, liquid NH_3 and MeOH production. For liquified H_2 production, input data for the H_2 liquefaction plant and H_2 loss are taken from Wulf and Zapp (2018) with a median electricity consumption of 10.5 kWh per kg of liquified H_2 (Al Ghafri et al., 2022). The LCI for liquid NH_3 production is derived from the research of

D'Angelo et al. (2021). The LCI for MeOH production comes from González-Garay et al. (2019). CO_2 feedstock is obtained via DAC, with its LCI provided by Keith et al. (2018).

2.2.4. Propulsion systems

The components in different propulsion systems vary from one another. Each component is sized according to the same output power required for the propeller and auxiliary systems. For the dual-fuel ICE combusting H_2-based fuels, 5 % of the energy content is required as MGO for pilot fuel (Kanchiralla et al., 2023). To reduce nitrogen oxide emissions in compliance with IMO Tier III regulations, selective catalytic reduction (SCR) is equipped on both main and auxiliary engines operating with HFO, liquid NH_3, and MeOH. For liquid H_2, however, SCR is applied only to the main engine. This is because H_2 combustion in the main engine can generate nitrogen oxides (NO_x), as the higher flame temperatures promote thermal NO_x formation from nitrogen and oxygen in the intake air, whereas such conditions are less pronounced in the auxiliary engine (Gao et al., 2021, EMSA, 2008). The activating element in the SCR catalyst is assumed to be TiO_2, making up about 0.25 % of the SCR weight (Liang et al., 2011). SCR catalysts are expected to be replaced once during the ship's lifetime (Kanchiralla et al., 2022).

The specific components for different propulsion systems are detailed in the SI Figure S1. Key parameters and LCI sources for these components are listed in Table S2 in the SI. For the LCI of motor drive manufacturing, material data is sourced from Westberg (2020) and electricity consumption information is from the manufacturer (ABB, 2003).

2.2.5. Fuel storage

The HFO is stored in normal diesel tanks (Kanchiralla et al., 2022). Liquid H_2 and NH_3 are stored in cryogenic tanks. MeOH, being liquid at room temperature, is stored in MeOH tanks. The characteristics of these fuels, their storage requirements, and the corresponding LCI sources are summarized in Table S3 in the SI.

2.2.6. Ship operation

Compared to HFO, H_2-based fuels have lower volumetric and gravimetric energy densities in onboard storage, either due to their inherently low energy density (e.g., liquid NH_3 and MeOH) or the need for dedicated cryogenic tanks with insulation (e.g., liquid H_2 and liquid NH_3). As a result, using all types of H_2-based fuels may necessitate sacrificing part of the cargo space and weight to complete the same voyage. The processes for determining these values are illustrated in Figure S2 in the SI. The detailed calculation process is discussed further in the subsequent sections.

To complete the same voyage with different propulsion systems and operating scenarios, the corresponding on-board energy demands are determined using Eq. (2).

$$E_{ij} = \left(\frac{P_{AM}}{\eta_{M_i}} + \frac{P_{AA}}{\eta_{A_i}}\right) \times T_j \times FM \tag{2}$$

whereE_{ij} is the total onboard energy demand of the ship range under the propulsion system i and operation scenario j, in MWh; P_{AM} and P_{AA} (see Eqs. (3)–(4)) are the average output power of the main engine and auxiliary power system, in MW; η_{M_i} and η_{A_i} are the efficiencies of the main engine and auxiliary power system for the propulsion system i; T is the sailing time in the operation scenario j, determined by the ship range and operating speed, hours; FM is the fuel margin (120 %(Hanssen et al., 2020)), introduced to ensure voyage completion even in the event of potential detours, unexpected bad weather conditions, or similar factors (Stolz et al., 2022).

The average output power of main and auxiliary engines is calculated according to Eqs. (3) and (4) IMO 2021b(IMO, 2021b)

$$P_{AM} = \frac{P_M \times \left(\frac{D_{Ave}}{D_{Max}}\right)^{\frac{2}{3}} \times \left(\frac{S_{Ave}}{S_{Max}}\right)^3}{\eta_w \times \eta_f} \tag{3}$$

where P_M is the installed power of the main engine, MW; D_{Max} and D_{Ave} are the maximum and average draught of the ship, respectively; S_{Max} and S_{Ave} are the maximum and average operating speed of the ship, respectively; η_w and η_f are correction factors for weather and fouling.

$$P_{AA} = P_A \times LF_A \tag{4}$$

where P_A is the installed power of the auxiliary engine, MW; LF_A is the average load factor of the auxiliary engine (50 % (MAN 2024, Perčić et al., 2022)).

For liquid H_2 and NH_3, boil-off gas (BOG) can occur when heat penetrates the cryogenic tanks. Although BOG can be utilized for propulsion, it is conservatively assumed to be reliquefied for better control (McKinlay et al., 2021). Since the BOG volume decreases as fuel is consumed, the reliquefaction system is designed based on the maximum hourly BOG volume. The additional energy required for BOG reliquefaction is calculated using Eq. (5).

$$E_{R_{ij}} = \frac{k_{R_{ij}}}{\lambda_{A_i}} \times \sum_{t=0}^{T-1} \left[\left(\frac{E_{ij}}{\rho_i} - \frac{E_{ij} \times t}{\rho_i \times FM \times T}\right) \times BOG_i\right] \tag{5}$$

where $E_{R_{ij}}$ is the energy demand for reliquefying BOG, in MWh; $k_{R_{ij}}$ is the electricity consumption for reliquefying the BOG of propulsion system i under operation scenario j, assumed as 3.3 kWh/kg for liquid H_2 (Lee et al., 2019) and 0.224 kWh/kg for liquid NH_3 (Lee et al., 2022); t is time point of ship operation in one voyage, in hours; ρ_i is the energy density for fuel used in propulsion system i; and BOG_i is the hourly evaporation rate of the fuel used in propulsion system i, assumed as 0.0167 % per hour for liquid H_2 and 0.0017 % per hour for liquid NH_3 (Song et al., 2022).

In addition to the variations in fuel volume and mass, and the corresponding tank sizes required by different propulsion systems, the installed power, volume, and mass of some components in H_2-based propulsion systems differ from those in traditional systems. Consequently, there will be changes in cargo space and weight, as described by Eqs. (6) and (7).

$$\Delta V_{ij} = \beta \times V_{OE} + V_{OT} + V_{OO} - \alpha \times V_{HE_i} - \left(E_{ij} + E_{R_{ij}}\right) \times \left(\frac{0.95}{V_{FT_{Hi}}} + \frac{0.05}{V_{FT_{Pi}}}\right) - V_{HO_i} \tag{6}$$

where ΔV_{ij} is the change in cargo space (in m^3) due to the adoption of H_2-based propulsion system i in the scenario j. β is the ratio of the engine room volume to the HFO-ICE main engine volume (V_{OE}), which is 5 times larger due to clearances required for access and maintenance (Minnehan and Pratt, 2017). V_{OT} is the volume of the existing HFO tank, which is 12,000 m^3. V_{OO} is the sum of volumes of other necessary components in the HFO-ICE propulsion system, m^3; α is the ratio of the engine room volume to the volume of the main engine in H_2-based propulsion system i (V_{HE_i}), which is 5 times larger for the dual fuel ICE (Minnehan and Pratt, 2017). $V_{FT_{Hi}}$ and $V_{FT_{Pi}}$ are volumetric energy densities (including tank) of the H_2-based fuel and pilot fuel used in the propulsion system i. V_{HO_i} is the sum volume of other components in the H_2-based propulsion system i.

$$\Delta M_{ij} = M_{OE} + M_{OT} + \frac{E_{ij}}{G_O} + M_{OO} - M_{HE_i} - \left(E_{ij} + E_{R_{ij}}\right) \times \left(\frac{0.95}{G_{FT_{Hi}}} + \frac{0.05}{G_{FT_{Pi}}}\right) - M_{HO_i} \tag{7}$$

where the ΔM_{ij} is the change in cargo weight (in tons) due to the

replacement of the HFO-ICE propulsion system with the H_2-based propulsion system *i* in the scenario *j*. M_{OE} is the mass of the HFO main engine andM_{OT} is the mass of the existing HFO tank. G_O is the gravimetric energy density of HFO. M_{OO} is the sum mass of other components in the HFO-ICE system. M_{HE_i} is the mass of the main engine of the H_2-based propulsion system *i*. $G_{FT_{Hi}}$ and $G_{FT_{Pi}}$ are gravimetric energy densities (including the tank) of the H_2-based fuel and pilot fuel used in the propulsion system *i*. M_{HO_i} is the sum mass of other components in the propulsion system *i*.

Finally, the fuel consumption per t-nm is determined based on the energy demand leaving the fuel margin, ship range and resulting cargo weight. The emissions with different propulsion systems are detailed in Table S4 in the SI.

2.2.7. Background data

To avoid the temporal mismatch between foreground and background data and to reflect the future development in other key sectors, this study uses prospective LCI background databases. These are derived from ecoinvent v3.8 database (system model "Allocation, cut-off by classification") (IRENA, 2021b) and the REMIND model (Baumstark et al., 2021), utilizing the open-source Python library premise v1.5.8 (Sacchi et al., 2022). The REMIND model provides global future scenarios based on shared socioeconomic pathways (SSPs) and representative concentration pathways. For the STEPS and NZE scenarios, two prospective LCI databases are used: SSP2-NDC (~2.5 °C warming by 2100) and SSP1-PkBudg500 (~1.3 °C warming by 2100). These databases update electricity inventories to reflect the regional electricity mix and efficiencies of various technologies, including CCS and photovoltaic panels (Lamers et al., 2023).

The Activity Browser (Steubing et al., 2020), an open source LCA software was used for LCI modeling and LCA calculations. Multiple foreground scenarios and prospective LCI background databases were handled by the superstructure approach (Steubing and de Koning, 2021).

2.3. Life cycle impact assessment

To quantify the climate change (kg CO_2-eq) impact, based on the IPCC AR5 characterization factors of global warming potentials with a time horizon of 100 years (IPCC, 2013), we add characterization factors for the uptake and release biogenic CO_2 (-1 and +1 respectively), which is needed to account for technologies such as bioenergy with CCS, and H_2 (+11), as H_2 can act as an indirect greenhouse gas (Warwick et al., 2022). Additionally, 15 other environmental impact categories are assessed using the method of Environmental Footprint v3.0 (Fazio et al., 2018). These categories include acidification (mol H+-eq), ecotoxicity: freshwater (CTUe), resource use: energy carriers (MJ), eutrophication: aquatic freshwater (kg P-eq), eutrophication: aquatic marine (kg N-eq), eutrophication: terrestrial (mol N-eq), human toxicity: cancer effects (CTUh), human toxicity: non-cancer effects (CTUh), ionizing radiation: human health (kBq U^{235}), land use (dimensionless), resource use: minerals and metals (kg Sb-eq), ozone depletion (kg CFC-11-eq), particulate

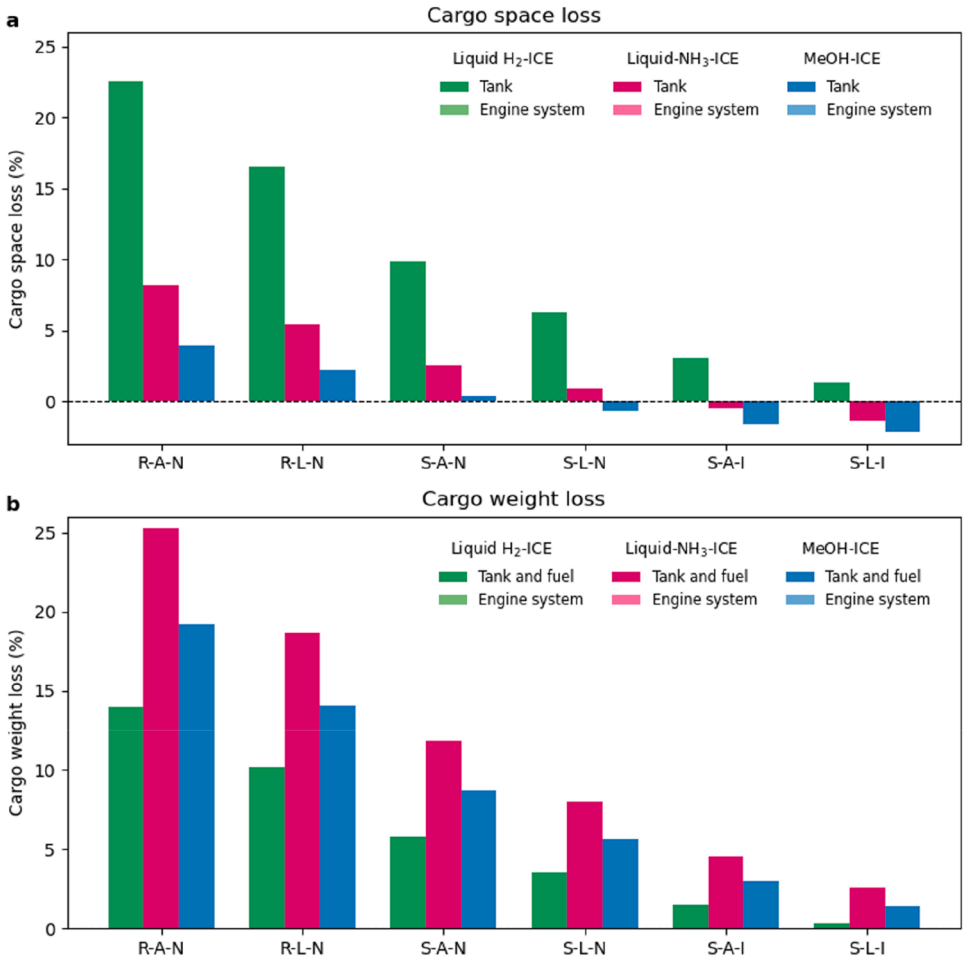

Fig. 2. The cargo space and weight losses associated with H_2-based propulsion systems compared to the traditional one. In this figure, R-A-N = 22,000 nm-20 knots-Nonstop, R-L-N = 22,000 nm-16 knots-Nonstop, S-A-N = 11,000 nm-20 knots-Nonstop, S-L-N = 11,000 nm-16 knots-Nonstop, S-A-I = 5500 nm-20 knots-1 refueling stop, and S-L-I = 5500 nm-16 knots-1 refueling stop. It should be noted that the cargo space and weight change caused by the engine system are minimal, at most 0.02 %, which makes them negligible.

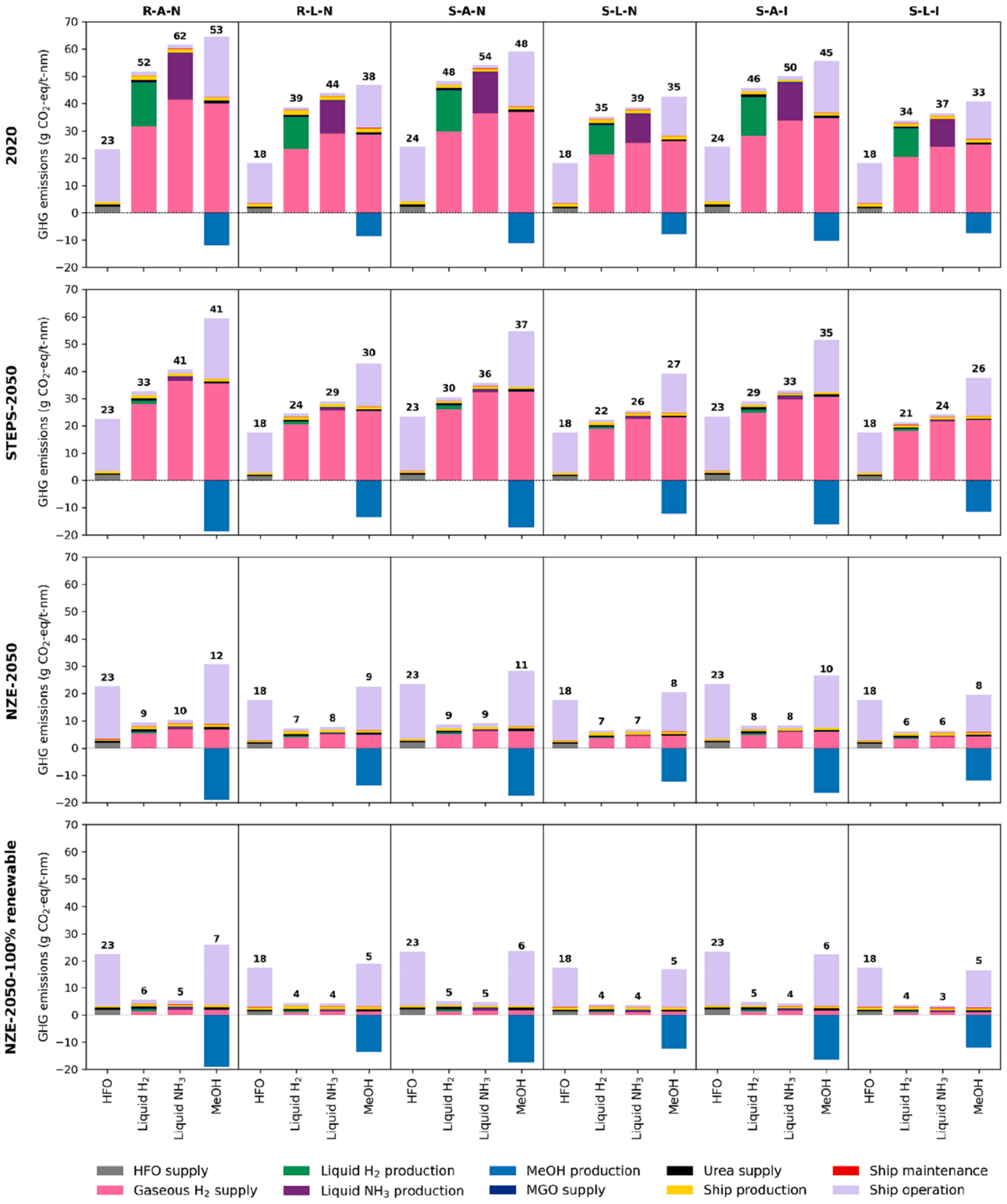

Fig. 3. The process contribution to the GHG emissions per t-nm of different ships in different scenarios. For the liquid H_2 production, liquid NH_3 production and MeOH production, the gaseous H_2 supply is a part of them and presented separately. In this figure, R-A-N = 22,000 nm-20 knots-Nonstop, R-L-N = 22,000 nm-16 knots-Nonstop, S-A-N = 11,000 nm-20 knots-Nonstop, S-L-N = 11,000 nm-16 knots-Nonstop, S-A-I = 5500 nm-20 knots-1 refueling stop, and S-L-I = 5500 nm-16 knots-1 refueling stop. For the MeOH-ICE case, the negative value is caused by the direct air capture. The GHG emissions per t-km are also provided in Figure S3 in the SI for comparison with other land-based transport.

matter (disease incidences), photochemical ozone formation (kg NMVOC-eq) and water use (kg world eq. deprived).

3. Results and discussion

3.1. Cargo space and weight loss

The cargo space and weight loss caused by using H_2-based propulsion system use are shown in Fig. 2. Regardless of cargo space or mass loss, fuel storage remains the primary factor, while the impact of the propulsion system is negligible. For cargo space loss, the liquid H_2 system results in the greatest cargo space loss due to its lowest volumetric energy density among the three fuels. In the typical scenario (S-A-N), the cargo space loss is 10 %. Longer ranges exacerbate this loss, as a larger fuel storage capacity is required; for instance, doubling the range (scenario R-A-N) can lead to up to 23 % cargo space loss. NH_3 and MeOH have less severe impacts. In the R-A-N scenario, MeOH requires only 4 % more space compared to the traditional propulsion system. If interim port calls are possible (scenarios S-A-I and S-L-I), container ships powered by liquid NH_3 and MeOH will require smaller tanks than HFO-powered ships, allowing for 1 % and 2 % more cargo space, respectively. It should be noted that although the cargo space loss is significant, unlike the mass constaint, it can be alleviated by placing the tank on the deck (ABS, 2021, IEA-AMF, 2013). For the cargo weight, alternative propulsion systems have adverse effects regardless of the fuel type. The trend in cargo weight loss by fuel type differs from that of cargo space loss. The liquid H_2 storage system has a higher gravimetric energy density compared to the liquid NH_3 and MeOH. Consequently, the cargo weight loss with a liquid H_2 system ranges from 0.3 % to 14 % across the S-L-I to R-A-N scenarios. Liquid NH_3 and MeOH reduce the cargo weight by 3–25 % and 1–19 %, respectively, across all scenarios.

The lower speed can reduce the energy demand of one voyage. For a single trip, lower speed can result in a 1–4 % reduction in cargo space loss and a 2–4 % reduction in cargo weight loss. In a round trip, lower speed shows a more significant impact, mitigating cargo space loss by 2–6 % and cargo weight loss by 4–6 %.

3.2. Prospective GHG emissions across H_2-markets

Fig. 3 illustrates the contribution of different processes to the GHG emissions of ships powered by HFO and H_2-based fuels. Currently, the case ship powered by HFO emit approximately 18–24 g CO_2-eq per t-nm, and its emissions are expected to remain unchanged in the future. For H_2-based ships, most of the emissions come from ship operation, H_2 supply, and liquid fuel production, which are correlated with the fuel and electricity used. Ship construction contributes only a small proportion, although some new equipment, such as cryogenic tanks or reliquefaction plants, may be required. In 2020, the GHG emissions from ships powered by H_2-based fuels are approximately 2–3 times higher than those from HFO ships across different scenarios. This is due to the significant reliance on fossil fuels in the electricity and H_2 production mix. For H_2 and NH_3 ships, aside from the emissions from H_2 supply, the main contributors to GHG emissions are the liquefaction process and the Haber-Bosch process, respectively. MeOH production can have negative GHG emissions due to CO_2 utilization from direct air capture, but its combustion releases CO_2. In the STEPS scenario, H_2-based fuel production benefits from electricity decarbonization, yet the H_2 market still heavily relies on fossil fuels. As a result, it is hard for ships that use H_2-based fuels to achieve GHG emission reduction compared to HFO-powered ships.

As electricity becomes increasingly decarbonized and the H_2 market shifts towards water electrolysis in the NZE scenario, the GHG emissions of H_2-based ships could drop to 6–10 g CO_2-eq per t-nm by 2050—35–52 % of those from HFO-powered ships. Even with long ranges, such as those outlined in the R-A-N scenario, GHG emissions do not show a significant increase compared to shorter single trips (S-A-N). Reducing speed and incorporating interim refueling stops have the potential to decrease the GHG emissions of H_2-powered ships by up to 26 % and 8 %, respectively. As a result, a non-stop voyage, paired with a lower speed, can achieve lower GHG emissions compared to adding an interim port call, as demonstrated in the S-L-N and S-A-I scenarios. Additionally, reducing speed can help mitigate the negative impact of cargo weight loss caused by the H_2-based propulsion system, without increasing the number of stops or the need for additional infrastructure.

In addition to using H_2 from the market, the shipping sector can also utilize green H_2 sourced from newly built renewable capacities to produce H_2-based fuels. This poses a challenge for the deployment speed of renewables (IEA, 2024), as it is a highly sought-after commodity by sectors beyond shipping. Here, we further modeled a 100 % renewable H_2-based fuel supply to quantify its environmental impacts on container shipping. We assume that all gaseous H_2 is produced entirely through proton exchange membrane electrolysis powered by onshore wind electricity. Additionally, subsequent processes such as H_2 liquefaction, the Haber-Bosch process, direct air capture and MeOH synthesis are also assumed to be powered by onshore wind electricity. When liquid H_2-based fuels are produced using 100 % onshore wind electricity, GHG emissions can be reduced by 75–79 %, 76 %–82 %, and 69 %–75 % by 2050 in the NZE scenario for liquid H_2, liquid NH_3, and MeOH, respectively. The GHG emissions of H_2-based ships powered by 100 %-renewable fuels is around 3–7 g CO_2-eq per t-nm. 100 % renewable H_2-based fuels can greatly mitigate the climate change impact of the shipping sector but may not fully achieve its net-zero target.

3.3. Prospective GHG emissions by H_2 sources

The S-A-N scenario is further used as an example to illustrate the GHG emissions of container ships powered by H_2-based fuels derived from various H_2 sources. As shown in Fig. 4, H_2-based fuels sourced from biomass and water electrolysis exhibit more significant changes over time compared to those produced directly from fossil fuels.

In 2020, only H_2-based fuels produced via biomass gasification with CCS offer significant GHG emission reductions compared to HFO. Although gaseous H_2 from biomass gasification currently results in very low emissions, the electricity demand for H_2 liquefaction and liquid NH_3 production leads to only slightly lower emissions for container ships fueled by liquid H_2 and NH_3 relative to HFO. In contrast, MeOH-ICE can achieve a 40 % reduction in GHG emissions compared to HFO. By 2050, H_2-based fuels from biomass gasification can reduce GHG emissions by 75–82 % compared to HFO. Despite this substantial potential, the share of biomass gasification in overall H_2 production is expected to remain marginal by 2050 (Wei et al., 2024). Concerns over large-scale deployment of bioenergy with CCS include socio-economic and environmental impacts due to intensive land, water, and nutrient requirements (Hanssen et al., 2020, Fujimori et al., 2022). In contrast, container ships powered by H_2-based fuels from water electrolysis using current grid electricity emit roughly three times more GHG than those using HFO, due to the fossil fuel-dominated electricity mix. As the grid electricity decarbonizes, GHG emissions from liquid H_2-ICE, liquid NH_3-ICE, and MeOH-ICE can decrease to 4–8 g, 3–8 g, and 5–10 g CO_2-eq per t-nm by 2050—representing reductions of 65–83 %, 64–86 %, and 57–79 %, respectively, compared to HFO. H_2-based fuels produced using solid oxide electrolysis cells exhibit higher GHG emissions than those from alkaline and proton exchange membrane electrolysis, primarily due to the external heat requirements in H_2 production.

For H_2-based fuels derived from fossil fuels, with or without CCS, emissions in 2020 remain higher than those from HFO. However, with electricity grid decarbonization, fossil-derived H_2 with CCS can reduce GHG emissions by 2050. Specifically, for fuels from coal gasification with CCS, GHG emissions can be reduced by 22 %, 11 %, and 3 % for liquid H_2-ICE, liquid NH_3-ICE, and MeOH-ICE, respectively. For fuels from natural gas steam reforming with CCS, reductions reach 39 %, 32 %, and 24 %, respectively, compared to HFO.

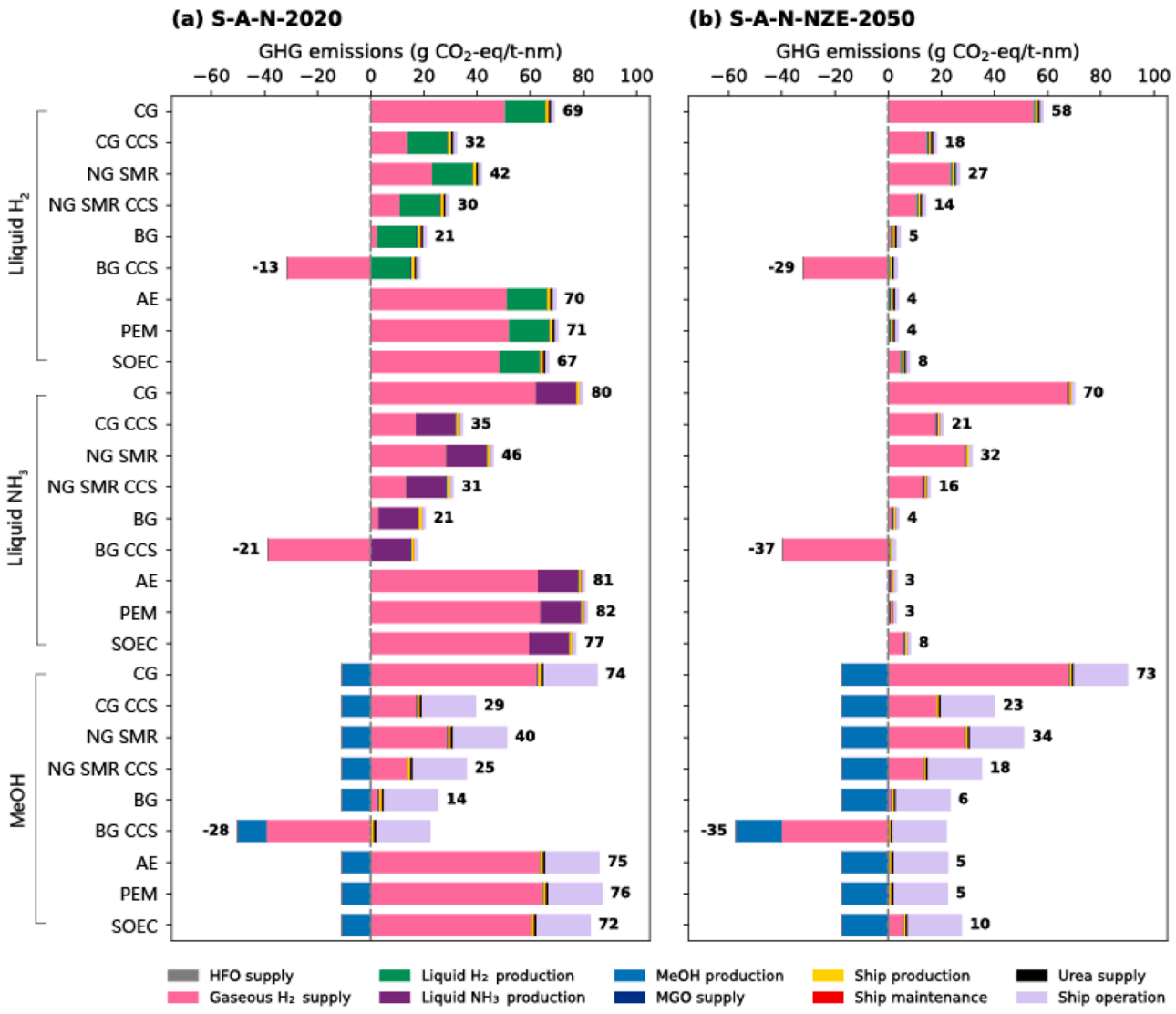

Fig. 4. Prospective GHG emissions of container ships powered by H_2-based fuels from various gaseous H_2 sources. (a) and (b) show the results for container ships operating non-stop over 11,000 nm at 20 knots in 2020 and 2050 under the NZE scenario, respectively. In this figure, CG = coal gasification, NG SMR = natural gas steam reforming, BG = biomass gasification, CCS = carbon capture and storage, AE = alkaline electrolyzers, PEM = proton exchange membrane electrolyzers, and SOEC = solid oxide electrolysis cells. Negative emissions arise from H_2 production through biomass gasification combined with carbon capture and storage, and from CO_2 captured via direct air capture.

3.4. Trade-offs with other impact categories

The environmental benefits of H_2-based fuels largely depend on the decarbonization of electricity and the transition in H_2 production. As shown in Fig. 5, H_2-based ships currently offer limited environmental benefits compared to the HFO ship, due to the fossil fuel dominated electricity and H_2 markets—except in the case of ozone depletion, where lower fossil-fuel hydrocarbon emissions during fuel production result in a relative advantage (Pozzer et al., 2020). Primarily due to lower sulfur dioxide (SO_2) emissions from ships powered by liquid H_2 and MeOH, these ships have a reduced impact on acidification. In contrast, the higher NO_x and NH_3 emissions during NH_3 production, along with NH_3 slip during liquid NH_3 ship operation, result in a higher acidification impact for liquid NH_3 ships compared to the HFO ship. As the electricity mix shifts towards more renewables by 2050 in the STEPS scenario—while the H_2 market remains dominated by coal gasification and natural gas steam reforming without CCS—the reduced share of coal-fired electricity and associated aluminium emissionsn give H_2-based ships an edge in ecotoxicity impact (Chen et al., 2024) compared to HFO ships. Additionally, lower emissions of non-methane volatile organic compounds create the potential for liquid-H_2 ships to lessen the impact on photochemical ozone formation. The significant decarbonization of electricity and the simultaneous transition of H_2 production towards water electrolysis in the NZE scenario together further enhances these environmental benefits. The liquid H_2 ship shows a slight decrease in fossil fuel depletion compared to the HFO ship, as fossil fuel-based H_2, most of which is produced with CCS, still accounts for 39 % of the H_2 market by 2050 in the NZE scenario. In contrast, ships powered by liquid NH_3 and MeOH exhibit higher fossil fuel depletion because their energy densities are lower than that of liquid H_2. As a result, more fuel needs to be combusted to produce the same power output, even though their energy requirements per kilogram in the production process are lower than those of liquid H_2.

While H_2-based ships can achieve deep decarbonization by 2050 under the NZE scenario, there are also concerns that the use of H_2-based fuels may exacerbate certain environmental impacts compared to HFO-powered ships. These impacts—such as freshwater eutrophication, particulate matter formation, terrestrial eutrophication, and marine eutrophication—show a decreasing trend in their relative magnitude compared to those of HFO ships, as electricity generation and H_2

Fig. 5. Environmental tradeoffs of H_2-based ships in different scenarios from 2020 to 2050 in the S-A-N (11,000 nm-20 knots-Nonstop) scenario. The value represents the ratio of the environmental impact of H_2-based ships to that of the HFO ship. Note the nature of the scale: impact reductions are values in between 0 and 1, while impact increases are values from >1 to infinity.

production become increasingly decarbonized. For freshwater eutrophication, the impact decreases as the share of electricity and H_2 sourced from coal declines, because coal mining generates spoil that requires treatment and causes associated phosphate emissions to water. However, large-scale water electrolysis powered by renewable electricity requires significant amounts of copper, multi-silicon wafers, and steel in power generation equipment. The production of these materials involves direct and indirect phosphate emissions, which causes H_2-based ships to retain a higher freshwater eutrophication impact compared to HFO ships. Although the combustion of H_2-based fuels results in lower emissions of particulate matter, NO_x, and SO_2 than HFO, emissions from the production of H_2-based fuels lead to higher overall particulate matter formation. Replacing coal gasification with water electrolysis for H_2 production alleviates this impact to some extent. Nevertheless, the production of materials used in solar panels and wind turbines—such as aluminum, multi-silicon wafers, and steel—also emits particulate matter, NO_x, and SO_2. Even when electricity is entirely sourced from onshore wind, the high electricity demand of H_2-based fuels makes it difficult for them to have an advantage over HFO ships in terms of particulate matter formation. It should also be noted that NO_x and NH_3 emissions can contribute to particulate matter formation (Gu et al., 2021). The relatively high NO_x and NH_3 emissions in liquid ammonia production, along with higher NH_3 slip during ship operation, result in liquid NH_3-powered ships having the highest particulate matter formation impact among all H_2-based ships. For terrestrial and marine eutrophication, the impacts during the ship operation phase are similar between H_2-based and HFO-powered ships, as NO_x emissions are the primary contributor. The overall eutrophication impact is determined largely by the fuel supply. For liquid H_2 and MeOH, electricity use is the main source of NO_x and NH_3 emissions. In contrast, the production of liquid NH_3 involves higher emissions of these pollutants, resulting in the highest eutrophication impacts among the fuels considered.

Simultaneously, environmental pressures such as mineral and metal extraction, land and water use, ionising radiation, and human toxicity are intensifying due to decarbonization efforts in the electricity and H_2 markets. As the deployment of renewables and water electrolysis expands, the growing demand for rare earth metals needed for solar panels (e.g., tellurium and indium), wind turbines (e.g., neodymium and dysprosium), and electrolyzers (e.g., platinum and iridium) (Luderer et al., 2019, Minke et al., 2021) increases the need for metal and mineral extraction. The installation of new infrastructure also exacerbates competition for land use. Additionally, as H_2 production increasingly relies on water electrolysis, the water use impact of H_2-based ships also rises. Among H_2-based fuels, NH_3 has the highest water use impact due to water evaporation in the cooling tower during the cooling process of liquid NH_3 production. For ionizing radiation, the carbon-14 released

during the treatment of low-level radioactive waste via plasma torch incineration in petroleum production contributes to the impact associated with HFO ships. Similarly, natural gas extraction—used as a feedstock for H_2 production—also emits carbon-14, akin to petroleum production. More importantly, the electricity consumption in H_2-based fuel production significantly increases the ionizing radiation impact of H_2-based ships, as nuclear power contributes through radon-222 emissions from uranium tailings treatment, as well as carbon-14 emissions from the treatment of both low-level radioactive waste in uranium production and spent nuclear fuel. As a result, H_2-based ships exhibit a higher ionizing radiation impact than HFO ships. The extent of water electrolysis expansion in the H_2 market and the reduction in nuclear power's share in the electricity mix from 2020 to 2050 affect this impact differently across scenarios: ionizing radiation decreases in the STEPS scenario, but increases in the NZE scenario by 2050 compared to 2020. For human toxicity with cancer effects, despite the production of HFO produces carcinogens such as benzo(a)pyrene, chromium and chromium VI, the ship production process is the major contrbuter for this impact due to low-alloyed and stainless steel use, which also emits above carcinogens. For the H_2-based ships, the large use of low-alloyed and stainless steel induced by liquid H_2 and NH_3 tanks as well as renewable electricity make the overall impact higher than the HFO ship. MeOH ship has the highest impact due to formaldehyde emissions during operation. For human toxicity with non-cancer effects, the fuel production and ship operation phases play decisive roles. In the case of the HFO ship, the impact is mainly attributed to chloride, lead, and mercury emissions during HFO production, as well as CO emissions during ship operation. In contrast, the production of H_2-based fuels requires significant amounts of electricity, which involves large-scale use of copper. Copper production is associated with emissions of arsenic, arsenic ions, cadmium, and lead, resulting in the higher impact for H_2-based ships compared to the HFO ship. Unlike liquid H_2 and NH_3 ships, which have lower CO emissions than the HFO ship, the MeOH ship emits more CO during operation, resulting in the highest impact among all ship types. Furthermore, using 100 % renewable H_2-based fuels can alleviate some environmental pressures, as onshore wind power has lower impacts in these categories compared to other grid electricity sources.

It should be noted although potential trade-offs associated with the use of H_2-based fuels may exist and have been discussed in this study, climate change remains a more relevant impact category due to the current contribution of shipping to global emissions. Moreover, most of the data in this study are focused on GHG emissions. Technological improvements and waste management strategies to reduce other environmental impacts not directly related to climate change were not considered. Therefore, our findings for other impact categories could involve both overestimations and underestimations, and should be seen as areas where potential improvements are needed.

4. Conclusions

In this study, by integrating the design for a typical Post-Panamax container ship with broader energy scenarios, the life cycle environmental impacts of using H_2-based fuels in internal combustion engines from 2020 to 2050 are quantified and compared with conventional HFO. The assessment framework established in this study comprehensively accounts for the impacts of H_2-based fuel use on cargo capacity changes, ship operation mode variations, and the decarbonization of electricity and H_2 markets. The results can provide policymakers with a more comprehensive view of the environmental benefits and risks associated with decarbonization through H_2-based fuels. The main conclusions are as follows:

The impact of using H_2-based fuels on ship cargo capacity depends on the ship's operating mode and fuel choice. For trips without any interim stops to refuel, using H_2-based fuels for container ships always requires sacrificing cargo space and weight, regardless of the fuel choice. This can result in a reduction of up to 10 % in cargo space and 12 % in cargo weight on a typical single trip without stop. Unless freight rates are sufficiently high to compensate for this effect, ship operations could become uneconomical. Specifically, liquid H_2 ships need to increase freight rates based on cargo volume, while liquid NH_3 and MeOH ships need to enhance rates based on cargo weight. When interim refueling is available, liquid NH_3 and MeOH ships can recover some cargo space. When using H_2-based fuels in internal combustion engines to decarbonize container ships, adjusting the operating mode and selecting appropriate fuel types are necessary to balance economic benefits.

H_2-based fuels could reduce GHG emissions from container ships by up to 65 % by 2050 under the NZE scenario, and by >80 % under a 100 %-renewables scenario. The source of H_2 supply is a crucial factor in determining whether H_2-based ships can effectively reduce GHG emissions compared to HFO ships. According to current policies, H_2-based ships cannot reduce GHG emissions by 2050, but under the NZE scenario with large-scale low-carbon water electrolysis, they could achieve substantial reductions. Among the options, liquid H_2-ICE shows the greatest potential for GHG reduction per t-nm. Moreover, if H_2-based fuels are produced from 100 % renewable electricity (here analyzed for onshore wind power), GHG emissions could be reduced by up to 82 %. Lowering ship speeds and incorporating interim refueling can further reduce GHG emissions, though their impact diminishes as H_2-based fuels become cleaner. From a long-term perspective, prioritizing the decarbonization of H_2 supply through water electrolysis over CCS is crucial for achieving deep decarbonization in shipping.

H_2-based fuels come with other environmental trade-offs compared to HFO, and these impacts need to be minimized. Decarbonizing containerships by replacing HFO with H_2-based fuels consistently reduces environmental impacts such as freshwater ecotoxicity and ozone depletion. However, H_2-based fuels tend to increase environmental burdens across most assessed categories, with metal and mineral use being the most significant due to reliance on renewables and water electrolysis. For eutrophication, human toxicity with non-cancer effects, and particulate matter formation, the main contributors are pollutants associated with the production of copper, aluminium, steel, and multicrystalline silicon wafers used in renewbale electricity equipment. Human toxicity with cancer effects is further influenced by the production of alloyed steel in ship production. These impacts should be mitigated through the development of advanced, efficient, and cost-effective pollutant removal technologies targeting these key materials.

Overall, achieving deep decarbonization of container ships with H_2-based fuels in ICEs requires water electrolysis sourced from renewables to develop faster than in the NZE roadmap, while carefully considering environmental trade-offs.

Declaration of generative AI in scientific writing

During the preparation of this work the author(s) used OpenAI/ChatGPT in order to polish the language. After using this tool/service, the author(s) reviewed and edited the content as needed and take(s) full responsibility for the content of the published article.

CRediT authorship contribution statement

Shijie Wei: Writing – original draft, Visualization, Methodology, Investigation, Funding acquisition, Data curation, Conceptualization. **Fayas Malik Kanchiralla:** Writing – review & editing, Methodology. **Frederik Schulte:** Writing – review & editing, Resources. **Henk Polinder:** Writing – review & editing. **Arnold Tukker:** Writing – review & editing, Supervision, Conceptualization. **Bernhard Steubing:** Writing – review & editing, Supervision, Conceptualization.

Declaration of competing interest

The authors declare that they have no known competing financial

interests or personal relationships that could have appeared to influence the work reported in this paper.

Acknowledgments

The authors thank the experts who provided insightful suggestions that helped refine our analysis. This work is supported by the China Scholarship Council (GrantNo. 202006430008).

Supplementary materials

Supplementary material associated with this article can be found, in the online version, at doi:10.1016/j.resconrec.2025.108671.

Data availability

The data used in this study are provided in the supporting information.

References

ABB, 2003. ACS 6000 Medium Voltage AC Drive For Speedand Torque Control For Power of 3 MW to 27 MW Motors. ABB, Zurich.
ABS, 2021. Setting the Course to Low Carbon Shipping: View of the Value Chain. American Bureau of Shipping, Texas.
Al Ghafri, S.Z.S., Munro, S., Cardella, U., Funke, T., Notardonato, W., Trusler, J.P.M., Leachman, J., Span, R., Kamiya, S., Pearce, G., Swanger, A., Rodriguez, E.D., Bajada, P., Jiao, F., Peng, K., Siahvashi, A., Johns, M.L., May, E.F., 2022. Energy Environ. Sci. 15, 2690–2731.
Balcombe, P., Brierley, J., Lewis, C., Skatvedt, L., Speirs, J., Hawkes, A., Staffell, I., 2019. Energy Convers. Manage. 182, 72–88.
Baumstark, L., Bauer, N., Benke, F., Bertram, C., Bi, S., Gong, C.C., Dietrich, J.P., Dirnaichner, A., Giannousakis, A., Hilaire, J., Klein, D., Koch, J., Leimbach, M., Levesque, A., Madeddu, S., Malik, A., Merfort, A., Merfort, L., Odenweller, A., Pehl, M., Pietzcker, R.C., Piontek, F., Rauner, S., Rodrigues, R., Rottoli, M., Schreyer, F., Schultes, A., Soergel, B., Soergel, D., Strefler, J., Ueckerdt, F., Kriegler, E., Luderer, G., 2021. Geosci. Model Dev. 14, 6571–6603.
Bicer, Y., Dincer, I., 2018. Int. J. Hydrogen Energy 43, 4583–4596.
Chen, Y., Fan, Y., Huang, Y., Liao, X., Xu, W., Zhang, T., 2024. Ecotoxicol. Environ. Saf. 269, 115905.
D'Angelo, S.C., Cobo, S., Tulus, V., Nabera, A., Martín, A.J., Pérez-Ramírez, J., Guillén-Gosálbez, G., 2021. ACS Sustain. Chem. Eng. 9, 9740–9749.
EMSA, 2008. Possible Technical Modifications On Pre-2000 Marine Diesel Engines for NO_x Reductions. European Maritime Safety Agency.
Fazio, S., Biganzioli, F., De Laurentiis, V., Zampori, L., Sala, S.D., 2018. E., *Supporting information to the Characterisation Factors of Recommended EF Life Cycle Impact Assessment methods, Version 2, from ILCD to EF 3.0*. European Commission, Ispra.
Fuhrman, J., Clarens, A., Calvin, K., Doney, S.C., Edmonds, J.A., O'Rourke, P., Patel, P., Pradhan, S., Shobe, W., McJeon, H., 2021. Environ. Res. Lett. 16, 114012.
Fujimori, S., Wu, W., Doelman, J., Frank, S., Hristov, J., Kyle, P., Sands, R., van Zeist, W.-J., Havlik, P., Domínguez, I.P., Sahoo, A., Stehfest, E., Tabeau, A., Valin, H., van Meijl, H., Hasegawa, T., Takahashi, K., 2022. Nat. Food 3, 110–121.
Gao, J., Xing, S., Tian, G., Ma, C., Zhao, M., Jenner, P., 2021. Fuel 285, 119210.
GMH, 2019. Efficiency Evaluation of Global 20 Major Container Ports. Global Maritime Hub.
González-Garay, A., Frei, M.S., Al-Qahtani, A., Mondelli, C., Guillén-Gosálbez, G., Pérez-Ramírez, J., 2019. Energy Environ. Sci. 12, 3425–3436.
Gu, B., Zhang, L., Van Dingenen, R., Vieno, M., Van Grinsven, H.J.M., Zhang, X., Zhang, S., Chen, Y., Wang, S., Ren, C., Rao, S., Holland, M., Winiwarter, W., Chen, D., Xu, J., Sutton, M.A., 2021. Science 374, 758–762.
Hanssen, S.V., Daioglou, V., Steinmann, Z.J.N., Doelman, J.C., Van Vuuren, D.P., Huijbregts, M.A.J., 2020. Nat. Clim. Chang. 10, 1023–1029.
ICCT, 2020. Refueling Assessment of a Zero-Emission Container Corridor between China and the United States: Could Hydrogen Replace Fossil Fuels? International Council on Clean Transportation.
IEA, 2024. The Role of E-fuels in Decarbonising Transport. International Energy Agency, Paris.
IEA-AMF, 2013. Alternative Fuels for Marine Applications. International Energy Agency-Advanced Motor Fuels, Wieselburg.
IMO, 2021a. The 2020 Global Sulphur Limit. International Maritime Organization.
IMO, 2021b. Fourth IMO GHG Study 2020. International Maritime Organization, London.
IMO, 2023. 2023 IMO Strategy on Reduction of GHG Emissions from Ships. International Maritime Organization.
IPCC, 2013. Climate Change 2013 – The Physical Science Basis: Working Group I Contribution to the Fifth Assessment Report of the Intergovernmental Panel On Climate Change. Intergovernmental Panel on Climate, Change, Cambridge. Report 9781107057999.
IRENA, 2021a. Innovation Outlook: Renewable Methanol. International Renewable Energy Agency.
IRENA, 2021b. A Pathway to Decarbonise the Shipping Sector By 2050. International Renewable Energy Agency, Abu Dhabi.
Jain, K.P., Pruyn, J.F.J., Hopman, J.J., 2016. Resour. Conserv. Recycl. 107, 1–9.
Kanchiralla, F.M., Brynolf, S., Malmgren, E., Hansson, J., Grahn, M., 2022. Environ. Sci. Technol. 56, 12517–12531.
Kanchiralla, F.M., Brynolf, S., Olsson, T., Ellis, J., Hansson, J., Grahn, M., 2023. Appl. Energy 350, 121773.
Keith, D.W., Holmes, G., St. Angelo, D., Heidel, K., 2018. Joule 2, 1573–1594.
Kim, K., Roh, G., Kim, W., Chun, K., 2020. Journal 8.
Korberg, A.D., Brynolf, S., Grahn, M., Skov, I.R., 2021. Renew. Sustain. Energy Rev. 142, 110861.
Lamers, P., Ghosh, T., Upasani, S., Sacchi, R., Daioglou, V., 2023. Environ. Sci. Technol. 57, 2464–2473.
Lee, H., Shao, Y., Lee, S., Roh, G., Chun, K., Kang, H., 2019. Int. J. Hydrogen Energy 44, 15056–15071.
Lee, J., Choi, Y., Choi, J., 2022. Journal 10.
Liang, Z., Ma, X., Lin, H., Tang, Y., 2011. Appl. Energy 88, 1120–1129.
Lindstad, H., Asbjørnslett, B.E., Strømman, A.H., 2011. Energy Policy 39, 3456–3464.
Luderer, G., Pehl, M., Arvesen, A., Gibon, T., Bodirsky, B.L., de Boer, H.S., Fricko, O., Hejazi, M., Humpenöder, F., Iyer, G., Mima, S., Mouratiadou, I., Pietzcker, R.C., Popp, A., van den Berg, M., van Vuuren, D., Hertwich, E.G., 2019. Nat. Commun. 10, 5229.
MAN, 2024. Propulsion Trends in Container Vessels. MAN Energy Solutions, Copenhagen.
McKinlay, C.J., Turnock, S.R., Hudson, D.A., 2021. Int. J. Hydrogen Energy 46, 28282–28297.
MI, 2019. What is The Speed of a Ship at Sea? Marine Insight.
Minke, C., Suermann, M., Bensmann, B., Hanke-Rauschenbach, R., 2021. Int. J. Hydrogen Energy 46, 23581–23590.
Minnehan, J.J., Pratt, J.W., 2017. Practical Application Limits of Fuel Cells and Batteries for Zero Emission Vessels. Sandia National Laboratories, United States.
Müller-Casseres, E., Leblanc, F., van den Berg, M., Fragkos, P., Dessens, O., Naghash, H., Draeger, R., Gallic, T.Le, Tagomori, I.S., Tsiropoulos, I., Emmerling, J., Baptista, L.B., van Vuuren, D.P., Giannousakis, A., Drouet, L., Portugal-Pereira, J., de Boer, H.-S., Tsanakas, N., Rochedo, P.R.R., Szklo, A., Schaeffer, R., 2024. Nat. Clim. Chang. 14, 600–607.
Notten, P.J., Althaus, H.-J., Burke, M., Läderach, A., 2018. Life Cycle Inventories of Global Shipping - Global. ecoinvent Association, Zürich.
A. Papanikolaou, Ship design - methodologies of preliminary design, 2014.
Perčić, M., Vladimir, N., Jovanović, I., Koričan, M., 2022. Appl. Energy 309, 118463.
Pozzer, A., Schultz, M.G., Helmig, D., 2020. Environ. Sci. Technol. 54, 12423–12433.
Sacchi, R., Terlouw, T., Siala, K., Dirnaichner, A., Bauer, C., Cox, B., Mutel, C., Daioglou, V., Luderer, G., 2022. Renew. Sustain. Energy Rev. 160, 112311.
Scheepvaartwest, 2025. Colombo Express - IMO 9295244. https://www.scheepvaartwest.be/CMS/index.php/containerships/9641-colombo-express-imo-9295244 (accessed 5th, February 2023).
M. Silva, Master, Norwegian University of Science and Technology, 2017.
Song, Q., Tinoco, R.R., Yang, H., Yang, Q., Jiang, H., Chen, Y., Chen, H., 2022. Carbon Capture Sci. Technol. 4, 100056.
SRI, 2018. Life Cycle Inventories of Global Shipping - Global. Sustainable Recycling Industries, Cape Town.
Steubing, B., de Koning, D., 2021. Int. J. Life Cycle Assess. 26, 2248–2262.
Steubing, B., de Koning, D., Haas, A., Mutel, C.L., 2020. Softw. Impacts 3, 100012.
Stolz, B., Held, M., Georges, G., Boulouchos, K., 2022. Nat. Energy 7, 203–212.
Terlouw, T., Treyer, K., Bauer, C., Mazzotti, M., 2021. Environ. Sci. Technol. 55, 11397–11411.
Tupper, E.C., 2013. In: Tupper, E.C. (Ed.), Introduction to Naval Architecture (Fifth Edition). Butterworth-Heinemann, Oxford, pp. 9–32. https://doi.org/10.1016/B978-0-08-098237-3.00002-3.
Warwick, N., Griffiths, P., Keeble, J., Archibald, A., Pyle, J., Shine, K., 2022. Atmospheric Implications of Increased Hydrogen use. Department for Business, Energy and Industrial Strategy.
Wei, S., Sacchi, R., Tukker, A., Suh, S., Steubing, B., 2024. Energy Environ. Sci. 17, 2157–2172.
Wernet, G., Bauer, C., Steubing, B., Reinhard, J., Moreno-Ruiz, E., Weidema, B., 2016. Int. J. Life Cycle Assess 21, 1218–1230.
E. Westberg, Independent thesis Advanced level (degree of Master (Two Years)) Student thesis, 2020.
Wulf, C., Zapp, P., 2018. Int. J. Hydrogen Energy 43, 11884–11895.